Polymer Degradation and Stability 98 (2013) 597–608

Contents lists available at SciVerse ScienceDirect

Polymer Degradation and Stability

journal homepage: www.elsevier.com/locate/polydegstab

Novel phosphorus-containing hyperbranched polysiloxane and its high performance flame retardant cyanate ester resins

Juhua Ye, Guozheng Liang*, Aijuan Gu*, Zhiyong Zhang, Jipeng Han, Li Yuan

Jiangsu Key Laboratory of Advanced Functional Polymer Design and Application, Department of Materials Science & Engineering, College of Chemistry, Chemical Engineering and Materials Science, Soochow University, Suzhou 215123, China

ARTICLE INFO

Article history:
Received 27 August 2012
Received in revised form
15 November 2012
Accepted 26 November 2012
Available online 1 December 2012

Keywords:
Phosphorus-containing flame retardant
Hyperbranched polysiloxane
Cyanate ester
Property

ABSTRACT

A novel phosphorus-containing hyperbranched polysiloxane (P–HSi) with a great amount of phosphaphenanthrene and silanol groups was synthesized by a hydrolysis of self-made phosphorus-containing triethoxysilane. Based on this, P–HSi was used to develop a new high performance flame retardant cyanate ester (CE) resin with simultaneously improved integrated properties. A small addition of P–HSi (5 wt%) to CE can remarkably increases the flame retardancy of CE resin, where the content of P element is only as low as about 1.8 wt%. More attractively, the incorporation of P–HSi to CE resin significantly improves the thermal stability and mechanical properties, completely overcoming the disadvantages of phosphorus flame retardants. Specifically, for the modified CE resin with 15 wt% P–HSi, its initial degradation temperature is about 58 °C higher than the corresponding value of original CE resin; moreover, its impact and flexural strengths are about 2.7 and 1.5 times of the corresponding values of CE resin, respectively. In addition, the P–HSi/CE resins have obviously decreased curing temperature and improved dielectric properties. These outstanding integrated properties of P–HSi/CE resins show that P–HSi is an effective and multi-functional flame retardant for developing high performance resins.

1. Introduction

High performance thermosetting resins with good flame retardancy are increasingly required by many cutting-edge industries including aerospace, microelectronic, and transportation, etc. [1–3]. However almost all resins do not have suitable flame retardancy.

To-date, adding flame retardant to a resin has been proved to be a common and effective method to endow the resin with good flame retardancy [4–6]. Phosphorus compounds become the main kind of flame retardants owing to their environment-friendly and high efficiency [7–9]. Among them, 9,10-dihydro-9-oxa-10-phosphaphenanthrene-10-oxide (DOPO) has received notable attention of scientists and engineers worldwide because of its additional merits such as good thermal stability, less toxicity, outstanding oxidation and water resistance [10–12]. Qian's group synthesized a new DOPO-containing flame retardant (HAP–DOPO) which was then used to modify epoxy resin, and found that the modified epoxy resin has higher char yield and lower heat release rate [13]. Our group prepared a novel modified bismaleimide (BMI) resin system by copolymerizing BMI with DOPO, and found that the modified BMI resin with a very low content of phosphorus element (1.25 wt%) has significantly improved flame retardancy [14]. Recently, Schartel's group published a series of papers on the flame redardancy and fire behavior of modified resins and carbon fiber-reinforced composites based on DOPO-containing flame retardants. They found that the flame retardancy of a resin is almost independent on the size of the flame retardants, but is closely related to the interaction between the DOPO-containing flame retardant and the resin, while the release of phosphorous compounds results in significant flame inhibition [15–18].

These researches prove that DOPO has a unique effect of improving the flame retardancy of resins. However, it is worthy to note that, compared with the original resin, the introduction of DOPO into the resin not only decreases the initial degradation temperature (T_{di}), leading to poor thermal stability, but also declines the mechanical properties (e.g. flexural strength) [19,20]. In fact, similar problems also exist in other phosphorus flame retardants [21–23]. Therefore, how to overcome these bottlenecks without worsening the advantages of DOPO is a very interesting issue.

* Corresponding authors. Tel.: +86 512 61875156; fax: +86 512 65880089.
E-mail addresses: lgzheng@suda.edu.cn (G. Liang), ajgu@suda.edu.cn (A. Gu).

0141-3910/$ – see front matter © 2012 Elsevier Ltd. All rights reserved.
http://dx.doi.org/10.1016/j.polymdegradstab.2012.11.015

Recently, our group synthesized a series of hyperbranched polysiloxanes, which were then used to prepared high performance thermosetting resins. Results show that the hyperbranched polysiloxane with a suitable structure will improve the integrated performance of the resin. A typical example is the fully end-capped hyperbranched polysiloxane with large branching degree and amine-groups (Am–HBPSi), its modified BMI resin simultaneously has improved flame retardancy, toughness, strength and thermal stability [24]. However, Am–HBPSi does not have a long-term storage stability owing to its high activity.

The paper reports the synthesis of a new phosphorus flame retardant, which is a phosphorus-containing hyperbranched polysiloxane with a great amount of DOPO and silanol groups (P–HSi); based on this, P–HSi was used to develop high performance flame retarding cyanate ester (CE) resin. CE resin was chosen as the base resin owing to its great potential in many cutting edges including electric and electronic industries, aerospace and aviation, etc. [25–27]. The effect of P–HSi on the structure and integrated performances (including curing behavior and mechanism, mechanical and dielectric properties, flame retardancy and the mechanism) were intensively investigated.

2. Experimental

2.1. Materials

CE used in this research was 2,2′-bis(4-cyanatophenyl)isopropylidene, which was bought from Jiangdu Resin Plant in China. Azobisisobutyronitrile (AIBN, 99.5%), ethanol, and concentrated hydrochloric acid (HCl, 36.5%) were purchased from Beijing Chemical Works, China. DOPO was obtained from Eutec Trading (Shanghai) Co. Vinyltriethoxy silane (VTES) was bought from Zhejiang Chem-tech Group Co., Ltd. Distilled water was produced in our lab.

2.2. Synthesis of P–HSi

The synthesis mechanism of phosphorus-containing hyperbranched polysiloxane with a great amount of DOPO and silanol groups (P–HSi) was shown in Fig. 1.

10 g VTES, 0.164 g AIBN and 10.8 g DOPO were added to a 500 mL reactor with a magnetic stirrer and a reflux condenser under a nitrogen atmosphere. The temperature was kept at 80 °C for 8 h to obtain a light yellow liquid, coded as DTES.

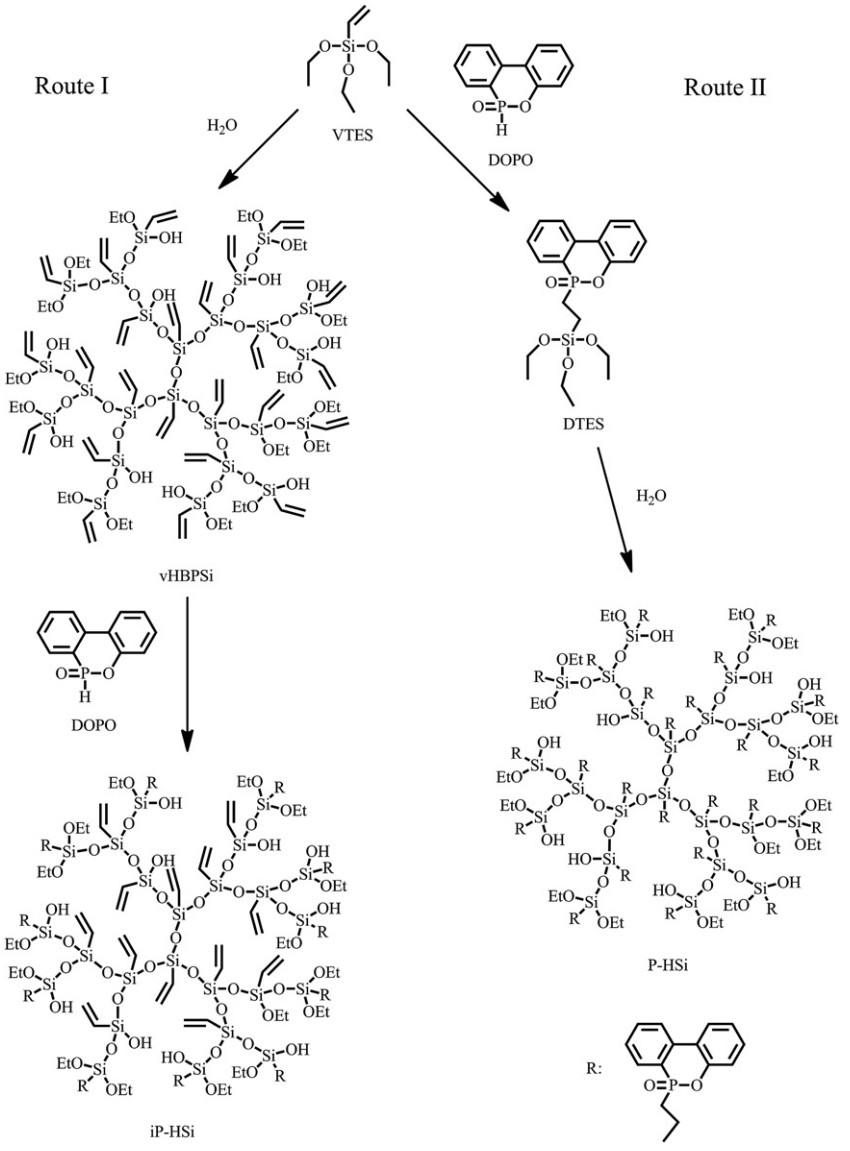

Fig. 1. Synthesis of iP–HSi and P–HSi.

10 g DTES and 12 g distilled water were put into another reactor to form a solution. HCl was slowly dropped into the reactor with stirring to adjust the pH value of the solution within the range between 2 and 3. After stayed at room temperature for 15 min, the solution was heated to 60 °C and maintained at that temperature with stirring for 2 h to get a crude product. The crude product was put into a vacuum oven to drive off ethanol, and then a transparent and viscous liquid was obtained, which was a hyperbranched polysiloxane with a great amount of DOPO and silanol groups, coded as P–HSi. The weight-average molecular weight (M_w) is 3200 g/mol.

2.3. Preparation of prepolymers and cured resins

Appropriate amounts of CE and P–HSi were thoroughly blended at 150 °C for 5 min with vigorous stirring to produce a prepolymer coded as P–HSi*x*/CE, where *x* means the weight loading of P–HSi in the prepolymer, taking values of 5, 10, 15, 20, 25, 30, and 35. A suitable amount of the prepolymer was put into an aluminum foil bag and cooled to room temperature for differential scanning calorimeter (DSC) tests.

The residual P–HSi*x*/CE prepolymer was degassed to remove entrapped air at 150 °C for 30 min, and then cast into a mold for curing and postcuring following the protocol of 180 °C/2 h + 200 °C/2 h + 220 °C/2 h, and 240 °C/4 h, successively, to get a cured P–HSi*x*/CE resin.

CE prepolymer and cured resin were also prepared using the procedures for P–HSi*x*/CE system except that no P–HSi was added.

2.4. Measurements

Fourier transform infrared (FTIR) spectra were recorded between 400 and 4000 cm^{-1} with a resolution of 2 cm^{-1} on a Prostar LC240 Infrared Spectrometer (USA).

^1H NMR and ^{31}P NMR spectra were recorded on a Bruker WM300 (Germany) with $CDCl_3$ as the solvent and internal standard.

^{29}Si NMR spectra were acquired at 99.36 MHz using 128 scans on a Bruker 500 MHz instrument (Germany) at 25 ± 2 °C. A 5 s delay time was used. Chromium (III) acetylacetonate with a concentration of 1 wt% was used as a paramagnetic relaxation agent to promote the rapid relaxation of the ^{29}Si nucleus.

Gel permeation chromatography (GPC) measurements were performed at 35 °C with tetrahydrofuran as the eluant (1.0 mL/min), and polystyrene as the standard using an Agilent 1100 system (USA).

DSC measurements were conducted on a DSC 2010 (TA Instruments, USA) ranging from room temperature to 350 °C with a heating rate of 10 °C/min under a nitrogen atmosphere.

Thermogravimetric (TG) analyses were done on a TA Instruments SDTQ600 in the range from 25 to 800 °C under a nitrogen atmosphere with a heating rate of 10 °C/min.

The dielectric constant and loss were measured using a Broadband Dielectric Spectrometer (Novocontrol Concept 80, Germany) at room temperature. The dimensions of each sample were (25 ± 0.02) × (25 ± 0.02) × (3 ± 0.02) mm^3.

DMA scans were performed using TA DMA Q800 apparatus from TA Instruments (USA). A single cantilever clamping geometry was used. DMA tests were carried out from room temperature to 320 °C at a heating rate of 3 °C/min at 3 Hz.

Limited oxygen index (LOI) values were measured on a Stanton Redcraft Flame Meter according to ASTM D2863/77. The dimensions of each sample were (100 ± 0.02) × (6.5 ± 0.02) × (3 ± 0.02) mm^3.

3. Results and discussion

3.1. Synthesis and characterization of P–HSi

Two new phosphorus-containing hyperbranched polysiloxanes (designed as P–HSi and iP–HSi) can be synthesized by employing different routes as shown in Fig. 1. Using Route I, the temperature for the addition reaction between DOPO and hyperbranched polysiloxane (vHBPSi) is 80 °C, however, at that temperature a gelation tends to be formed, and thus leading to the failure of synthesizing iP–HSi.

This phenomenon does not appear in the Route II. On the other hand, P–HSi prepared through Route II has much more content of the phosphorus element than that through Route I, meaning that P–HSi will have a better flame retarding effect than the iP–HSi. Therefore Route II is chosen as the suitable procedure for synthesizing a hyperbranched polysiloxane with a great amount of DOPO and silanol groups.

P–HSi is a slightly viscous liquid, which is completely miscible in any ratio with methanol, chloroform, toluene, tetrahydrofuran and hexane, etc.

Fig. 2 shows the FTIR spectra of DOPO, VTES, DTES and P–HSi. In the FTIR spectrum of DTES, the peak (2436 cm^{-1}) attributing to P–H groups of DOPO completely disappears, however some characteristic peaks assigning to phenyl (1479 cm^{-1}, 1431 cm^{-1}) and C–H (2881–2980 cm^{-1}) groups appear, indicating that DTES is the product of the reaction between DOPO and VTES. This statement can be confirmed by comparing the ^1H NMR spectra of VTES, DOPO and DTES shown in Fig. 3, specifically, the chemical shifts attributing to the $-CH{=}CH_2$ (5.67–6.29 ppm) and –H (8.70 ppm) groups appear in the ^1H NMR spectrum of VTES and DOPO, but not in the ^1H NMR spectrum of DTES; moreover, those representing phenyl (7.16–7.91 ppm) and $-CH_2-$ (0.87 ppm, 2.12 ppm) groups can be found in the ^1H NMR spectrum of DTES.

In the FTIR spectrum of P–HSi, there are the characteristic peaks belonging to Si–O–Si groups in the range of 1018–1166 cm^{-1}, suggesting that Si–OH groups were changed into siloxane; while the board peak centered at 3360 cm^{-1} representing Si–OH groups also can be observed, demonstrating that some Si–OH groups still exist after the hydrolysis. The emergence of the chemical shift at 2.78 ppm attributing to –OH groups in the ^1H NMR spectrum (Fig. 3) of P–HSi also supports this statement. Note that as observed by other researchers [28,29], the stretching vibration of P=O bond for DOPO appears as a sharp peak at 1238 cm^{-1}; while this peak (1238 cm^{-1}) can not be seen in the spectrum of P–HSi, instead,

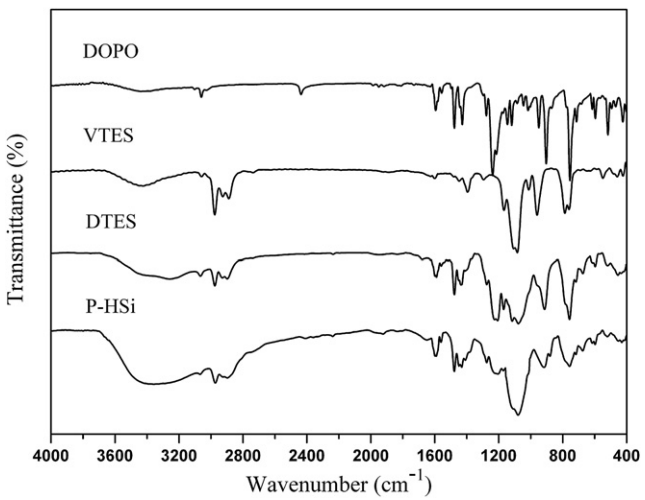

Fig. 2. FTIR spectra of DOPO, VTES, DTES and P–HSi.

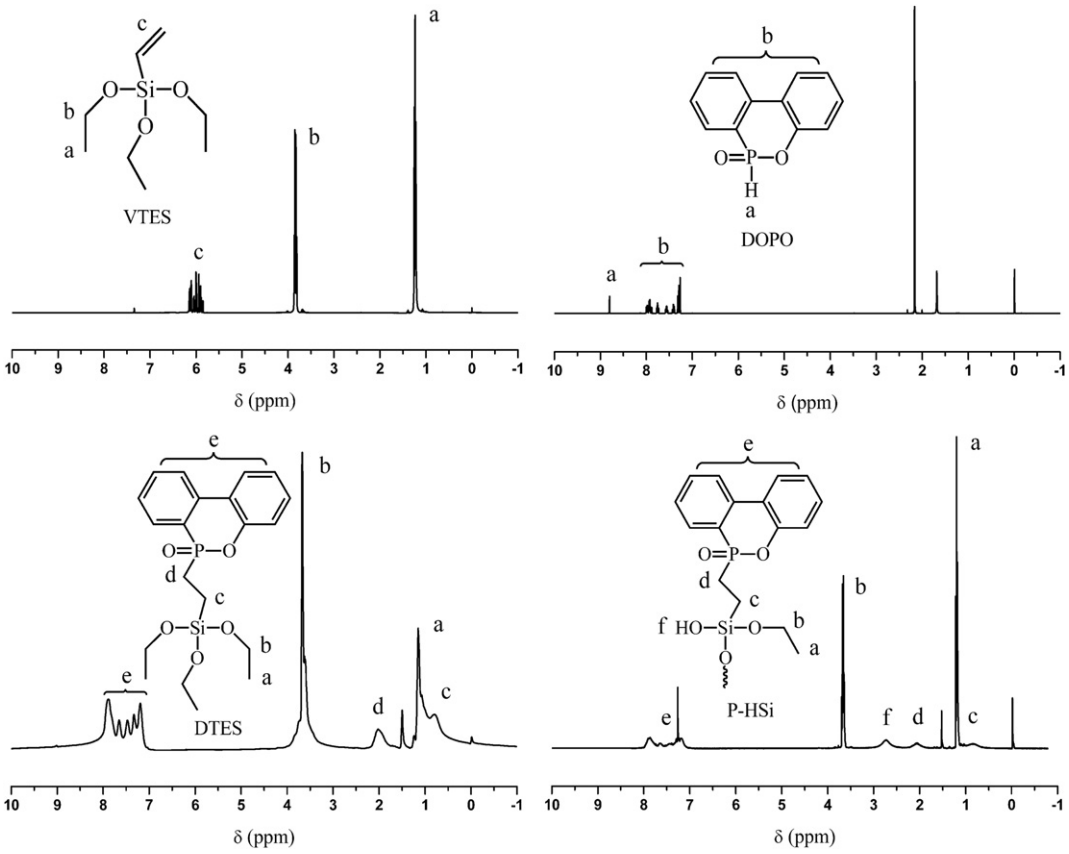

Fig. 3. ^{1}H NMR spectra of VTES, DOPO, DTES and P–HSi.

a small and wide peak appears in the range from 1185 cm^{-1} to 1258 cm^{-1}. Obviously, this results from the overlay of the stretching vibration of P═O bond and the peak nearby (1214 cm^{-1}). Using the peak fitting module of the Origin soft, the stretching vibration of P═O bond of P–HSi is at 1224 cm^{-1}. The shift in wave number and the change in the intensity of the peak demonstrate the formation of hydrogen bonds between P═O and –OH of P–HSi, similar results were also found between triphenylphosphine oxide (TPPO) and H_2O [30,31].

To further prove the existence of the hydrogen bonds in P–HSi, the temperature-dependent FTIR spectra of P–HSi at different temperatures were recorded as shown in Fig. 4. Because the Si–OH groups will co-react to liberate water as the temperature increases, hence the amount of –OH groups will decrease, and the stretching vibration of –OH gradually decreases and almost disappears at 200 °C. Therefore, only the variety of the stretching vibration of P═O bond can be used to evaluate the existence of the hydrogen bonds. It can be seen from Fig. 4 that as the temperature increases from 30 °C to 200 °C, the stretching vibration of P═O gradually shifts from 1224 cm^{-1} to 1235 cm^{-1}. This variety of the stretching vibrations of –P═O clearly reflects that there are hydrogen bonds between –OH and –P═O as the hydrogen bond decreases with the increase of temperature [32,33].

Fig. 5 shows the ^{31}P NMR spectra of DOPO, DTES and P–HSi. In the ^{31}P NMR spectrum of DTES, there is the peak (ca. 40.12 ppm) assigning to P–CH_2, but that at 14.82 ppm attributing to the P–H disappears, indicating the success of the reaction between DOPO and VTES. In the ^{31}P NMR spectrum of P–HSi, the chemical shift over the range from 39.70 to 43.96 ppm is broad because both terminal and dendritic units of P–HSi have P element, leading to slightly different environments of P elements [34].

Degree of branching (DB) and average number of branch units (ANB) are two important parameters for characterizing the branching structure of a hyperbranched polymer, they can be calculated according to Eqs. (1) and (2) [35] based on a ^{29}Si NMR spectrum.

$$DB = \frac{2D}{2D + L} \tag{1}$$

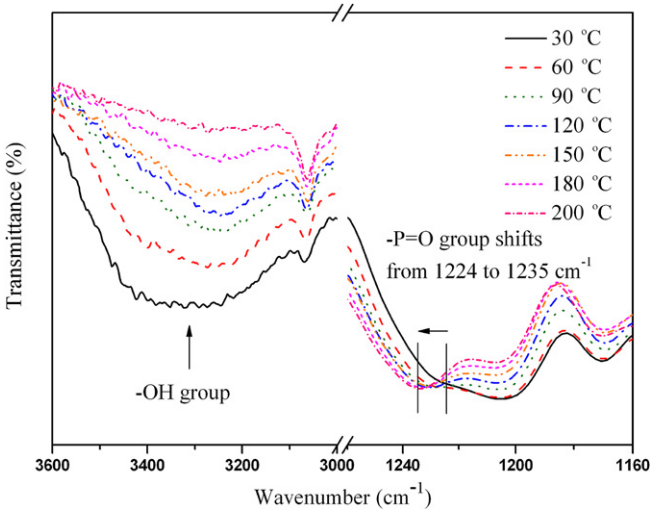

Fig. 4. The temperature-dependent FTIR spectra of P-HSi at different temperatures.

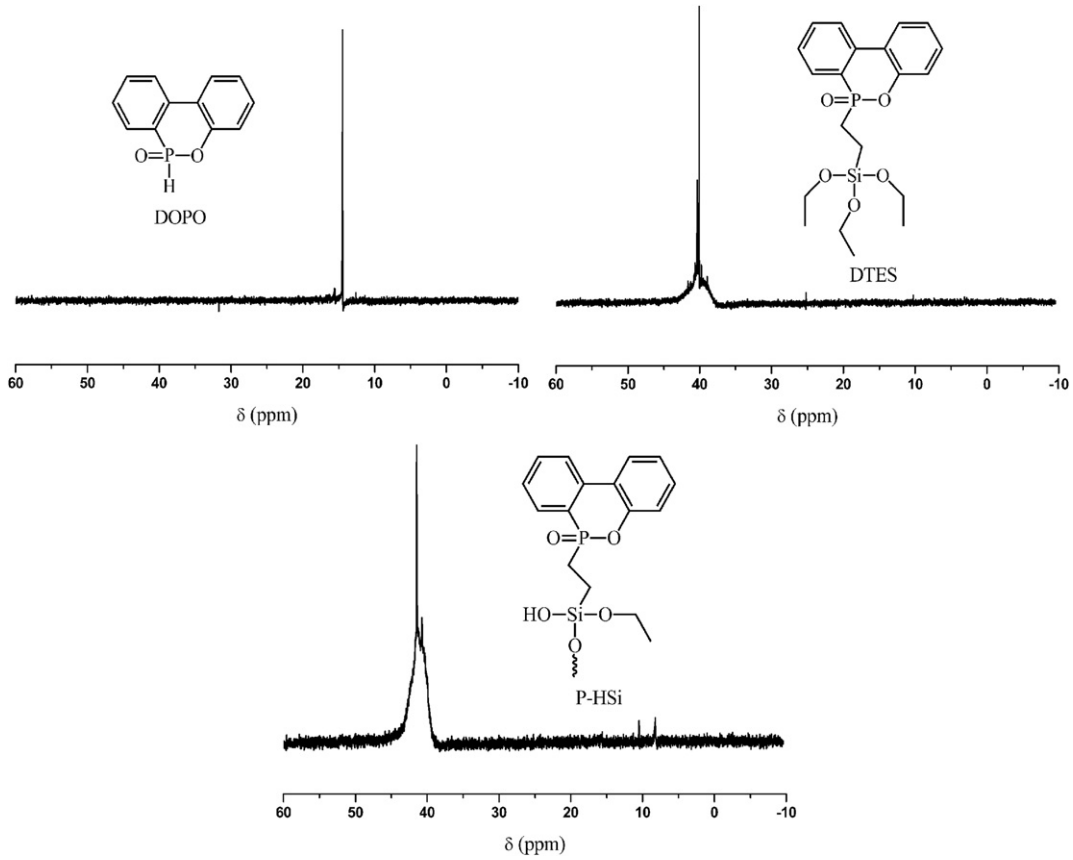

Fig. 5. ^{31}P NMR spectra of DOPO, DTES and P–HSi.

$$\mathrm{ANB} = \frac{D}{D+L} \tag{2}$$

where *D*, *L*, and *T* are the areas of the dendritic, linear, and terminal units, respectively.

The ^{29}Si NMR spectrum of P–HSi is shown in Fig. 6. The three chemical shifts at −75.80 ppm, −67.93 ppm and 59.30 ppm represent the dendritic, linear and terminal unit, respectively, and then the DB and ANB values are calculated to be 0.76 and 0.62, respectively.

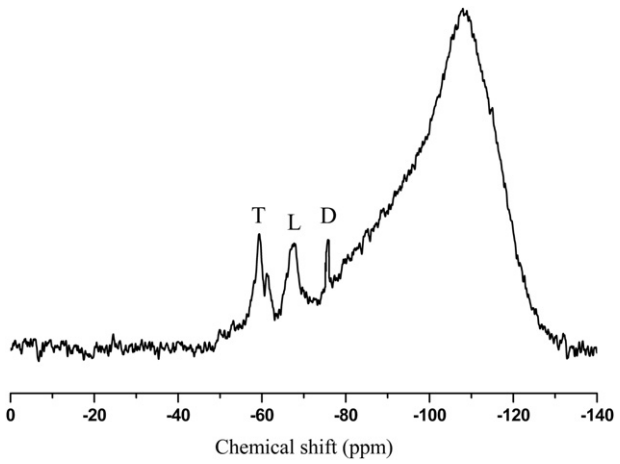

Fig. 6. The ^{29}Si NMR spectrum of P–HSi.

3.2. Crosslinked structure of cured P–HSi/CE resin

Macro-performance of a material is determined by its structure. For a thermosetting resin, its structure is divided into polymer chain and aggregation state structures, while the former can be reflected by the curing mechanism, and the latter can be characterized by the crosslinking density.

Fig. 7 depicts the DSC curves of CE and P–HSi/CE prepolymers. Each curve has an endothermic peak (at ca. 75 °C) and an exothermic peak, the former is the melting peak of CE monomer, while the latter represents the curing reaction. Note that the exothermic peak of P–HSi/CE shifts toward lower temperatures as the content of P–HSi increases, for example, the peak temperature of P–HSi10/CE is about 34 °C lower than that of CE, demonstrating that the addition of P–HSi changes the curing mechanism.

For CE resin, its main curing mechanism is the cyclotrimerization of –OCN to form crosslinked triazine rings [36]; while for P–HSi/CE system, besides above cyclotrimerization, there are additional reactions, including the chain extension [37] through the reaction between silanol groups in P–HSi and triazine rings (Fig. 8(a)) as well as the transesterification reaction [38] between ethoxyl and Ph-OH groups (Fig. 8(b)), and the condensation reaction [39,40] between Si–OH and Ph–OH groups (Fig. 8(b)). These reactions introduce flexible siloxane linkages into the cross-linked network.

On the other hand, as the content of P–HSi increases, the curing heat (ΔH) of the P–HSi/CE prepolymer significantly decreases

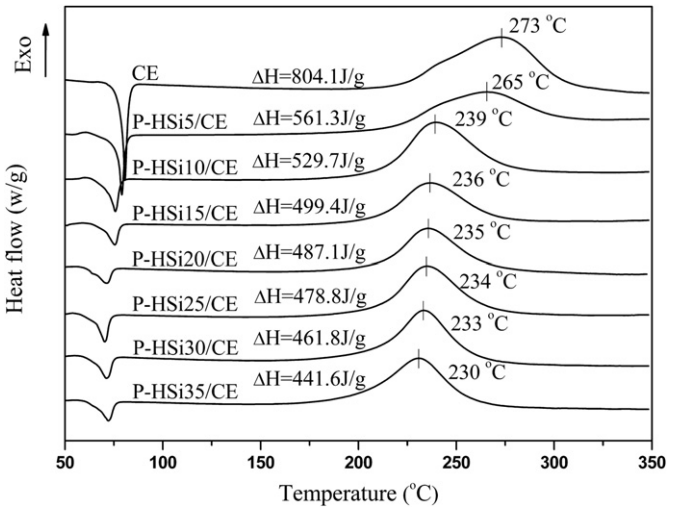

Fig. 7. DSC curves of CE and P–HSi/CE prepolymers.

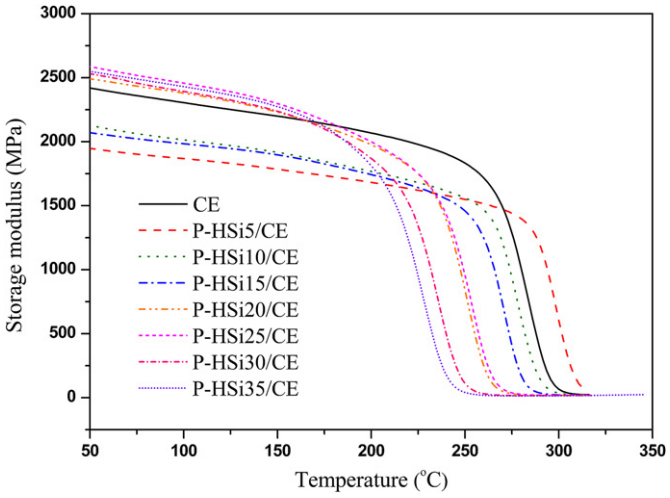

Fig. 9. Overlay curves of storage modulus as a function of temperature for cured CE and P–HSi/CE resins.

(Fig. 7). Especially, with the addition of only 5 wt% P–HSi into CE prepolymer, the curing heat reduces from 804.1 J/g to 561.3 J/g, only about 70% of that of CE prepolymer. P–HSi/CE prepolymers have lower curing heats than CE prepolymer, indicating that the incorporation of P–HSi to CE significantly changes the whole curing reaction from a strong reaction to a moderate one, meaning that the curing process becomes controllable by avoiding the heat accumulation and thermal explosion during cuing. This is a very attractive feature for fabricating materials, especially those with big thickness.

The crosslinking density ($X_{density}$), the concentration of crosslinking bonds per unit volume, of highly crosslinked systems can be calculated using a semi-empirical equation shown in Eq. (3) [41]:

$$\log_{10} G' = 7 + 293 X_{density} \quad (3)$$

where G' is the storage modulus (Fig. 9) of the cured resin in the rubbery plateau region above the glass transition temperature (T_g). Herein, G' is chosen as the modulus at the temperature that is 20 °C higher than T_g.

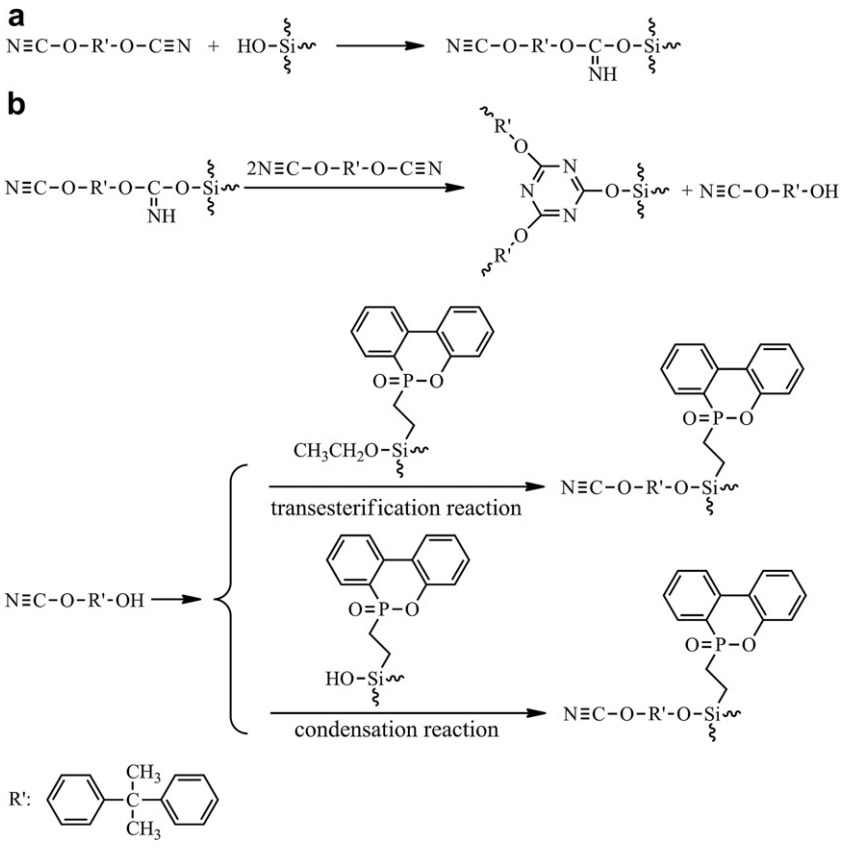

Fig. 8. Chemical reactions between P–HSi and CE.

Fig. 10 depicts the crosslinking densities of cured CE and P–HSi/CE resins. The content of P–HSi has obvious influence on the crosslinking densities of P–HSi/CE resins. As the content of P–HSi increases, the crosslinking density of P–HSi/CE resin slightly increases until reaches the maximum value at 15 wt%, and then obviously decreases. This originates from the curing mechanism and the unique topological structure of P–HSi. As discussed above that P–HSi/CE resins have lower curing temperature than CE, so the former can get bigger conversion than the latter. However, on the other hand, compared with the triazine rings network (for cured CE resin), which is a structure with big crosslinking density, there are additional long and flexible chains of P–HSi in the cured P–HSi/CE system, leading to a decreased crosslinking density. When the content of P–HSi is small, the positive factor is dominant, which is offset by the negative factor as the content of P–HSi increases.

3.3. Thermal property of cured P–HSi/CE resins

3.3.1. Thermal stability

Fig. 11 shows TG and DTG curves of cured CE and P–HSi/CE resins. The thermal degradation of each resin can be divided into two independent steps, of which the maximum degradation rate temperature (T_{max}) is about 445 °C and 515 °C, respectively, demonstrating that the original and modified CE resins have similar degradation processes. The corresponding T_{di} at which the weight loss of the sample reaches 5 wt%, the T_{max}, and char yield (Y_c) at 800 °C are summarized in Table 1. It can be seen that all resins have similar T_{max} values, indicating that the addition of P–HSi does not obviously change the chemistry of the majority of the molecular chains in each crosslinked network.

However, the T_{di} values of all P–HSi/CE resins are bigger than that of CE resin; while with the increase of the content of P–HSi, the T_{di} value of P–HSi/CE system initially increases until reaches the maximum value at 15 wt%, and then decreases. These attractive results demonstrate that P–HSi completely overcomes the disadvantage that the addition of DOPO and derivatives decreases the thermal stability of original resins as reported in literature. For example, Juang et al. found that the T_{di} value of epoxy resin modified by DOPO derivative is about 26 °C lower than that of original epoxy resins [42]. Wang's group observed that the addition of poly(DOPO-substituted hydroxy phenyl methanol pentaerythritol diphosphonate) into epoxy resin could decline the T_{di} value with a gap of about 63 °C [43]. The authors of these literature stated

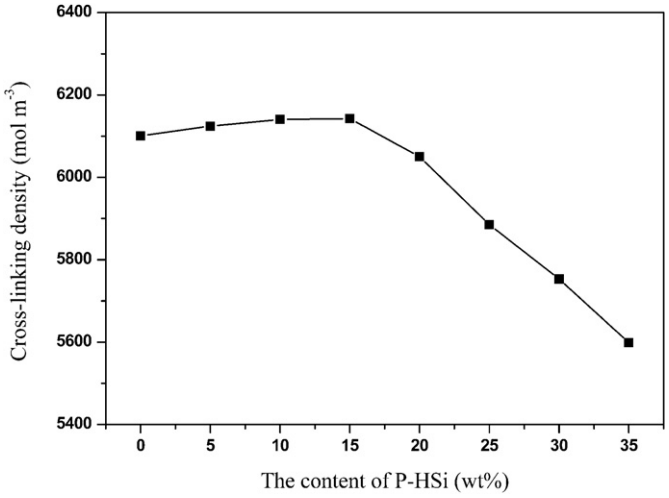

Fig. 10. Dependence of the content of P–HSi on the crosslinking density of cured CE and P–HSi/CE resins.

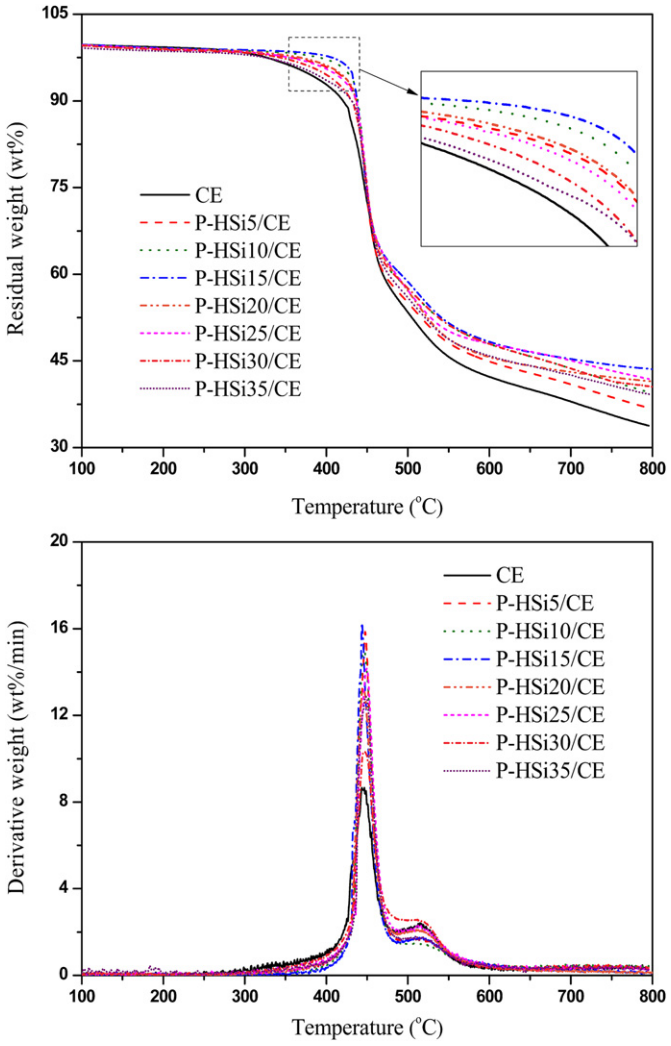

Fig. 11. TG and DTG curves of cured CE and P–HSi/CE resins.

that these decreased T_{di} values were attributed to the undesirable stability of O=P–O bond. Obviously, this viewpoint can not be used to explain the attractive data of P–HSi/CE system prepared herein, and it is believed that there are other factors that play positive roles in improving the T_{di} value.

T_{di} is usually used to evaluate the thermal stability of a material, which is sensitive to the bonds with the poorest thermal stability. The remarkable increase in the T_{di} value of P–HSi/CE resins demonstrates that the addition of P–HSi (especially when the content of P–HSi is not too large) into CE resin greatly enhances the

Table 1
Characteristic data from TG analyses of cured CE and P–HSi/CE resins.

Sample	T_{di} (°C)	T_{max} (°C)		Y_c at 800 °C (wt%)
		T_{max1}	T_{max2}	
CE	373	443	515	33.8
P–HSi5/CE	412	448	516	36.8
P–HSi10/CE	425	446	518	39.6
P–HSi15/CE	431	444	515	43.6
P–HSi20/CE	414	445	516	41.4
P–HSi25/CE	407	449	518	41.8
P–HSi30/CE	393	446	516	40.6
P–HSi35/CE	381	449	518	39.2

chemical bonds with the poorest thermal stability; in other words, the thermal stability of O=P–O bond is improved. This is reasonable as we have proved that there are hydrogen bonds between P=O and –OH of P–HSi in the above discussion of FTIR spectra.

In addition, some additional factors are also responsible for the increased T_{di} values. Compared with CE resin, the P–HSi/CE resins have additional Si–O–Si chains that have outstanding thermal stability [44], meaning that the concentration of the chains with relatively poor thermal stability decreases, leading to improved T_{di} values. In the case of P–HSi/CE resins, they have same chemistry but different crosslinking densities. As a bigger crosslinking density is beneficial to get a higher T_{di} [17], hence the influence of the content of P–HSi on the T_{di} value is the similar as that on the crosslinking density as discussed above.

On the other hand, the Y_c shows similar relation with the content of P–HSi as T_{di} does. It is known that Y_c reflects the ability to produce char at high temperature, hence the content of P–HSi has the similar effect on the T_{di} and Y_c.

Above discussion proves that P–HSi overcomes the drawback of the traditional phosphorus-containing flame retardants.

3.3.2. Glass transition temperature

Three methods are generally used to define T_g from DMA analysis [45], in this paper, the temperature corresponding to the loss modulus peak (Fig. 12) is considered as the T_g of materials.

It can be seen that each resin shows a strong and sharp peak, indicating that either original or modified resin has a single-phase structure. In the case of P–HSi/CE system, its T_g value increases initially and then decreases as the content of P–HSi increases, which is basically consistent with other hyperbranched polysiloxane modified resins [44,46] and DOPO contained resin [19,47]. The P–HSi/CE resin of which the content of P–HSi is not larger than 15 wt % has higher T_g value than CE resin. These data can be attributed to the combined result of multi-effects including the crosslinking density, hydrogen bond and hyperbranched structure of P–HSi.

Generally, higher crosslinking density and the formation of hydrogen bond are beneficial to restrict the molecular chain relaxation, leading to a higher T_g value. However, on the other hand, it's well known that a hyperbranched polymer generally exhibits spheroidical configuration, its branched molecular chains are too short to entangle and thus has big free volume [48]; in addition, Si–O–Si chains are flexible, so the presence of P–HSi tends to increase the motion ability of molecular chains.

3.4. Mechanical properties of P–HSi/CE resins

3.4.1. Impact strength

The impact resistance of a material reflects its ability to absorb the energy of a rapidly applied load, and the ability to withstand this sudden impact is related to the toughness of the material [49]. The impact strengths of cured CE and P–HSi/CE resins are presented in Fig. 13. All P–HSi/CE resins have higher impact strengths than CE resin. The impact strength of P–HSi/CE resins is greatly dependent on the content of P–HSi. As the content of P–HSi increases, the impact strength of P–HSi/CE resin initially increases and then reaches the maximum value (22.5 kJ/m^2) at 15 wt% P–HSi, which is about 2.7 times that of corresponding value of cured CE resin. This result is in good agreement with our previous researches on hyperbranched polysiloxane modified thermosetting resins [46,50–52].

From the curing mechanism of P–HSi/CE resins discussed above, it can be seen that the incorporation of P–HSi into CE resin introduces flexible siloxane linkages into the crosslinked network, and thus increasing the toughness. On the other hand, a large number of rigid pendant groups (benzene rings) offset some flexibility originated from siloxane linkages, hence the P–HSi/CE resin with a large content of P–HSi (>20 wt%) has a decreased toughness, however, this toughness is still greater than that of neat CE resin.

3.4.2. Flexural and storage moduli

Storage modulus (E') is related to the Young's modulus of the resin under periodic stress [53], which is an important parameter reflecting the stiffness of materials. The flexural modulus reflects the inherent energy of a material, and the ability to resist strain, moreover which is also a property reflecting the stiffness of a material [54]. Therefore, flexural and storage moduli are usually selected as typical parameters to evaluate the stiffness of the materials [54,55].

The overlay plots of E' as a function of temperature for cured CE and P–HSi/CE resins are shown in Fig. 9. There is one-step decrease in the E' of each resin. In the glassy state, as the content of P–HSi increases, the E' value of P–HSi/CE resins increases; when the content of P–HSi is larger than 15 wt%, the P–HSi/CE resin has higher E' values than neat CE resin. Similarly, the flexural moduli of the P–HSi/CE resins also follow the same dependence on the content of P–HSi (Fig. 14).

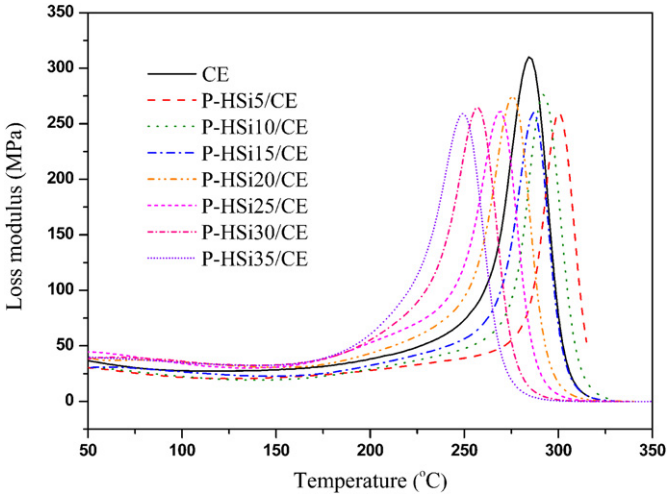

Fig. 12. Overlay curves of loss modulus as a function of temperature for cured CE and P–HSi/CE resins.

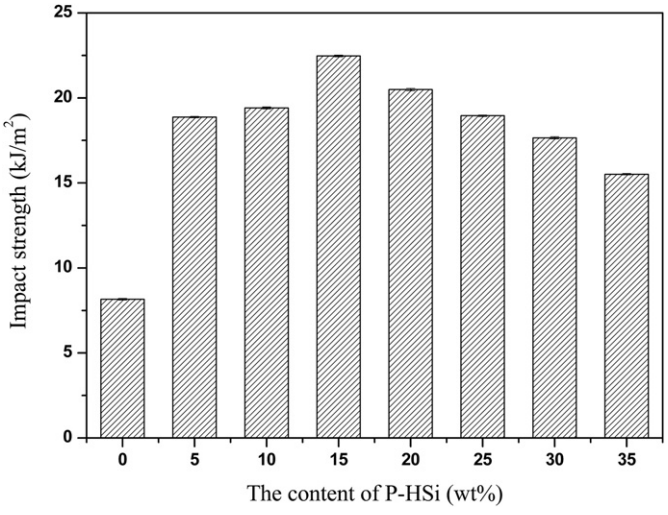

Fig. 13. Dependence of the content of P–HSi on the impact strength of cured CE and P–HSi/CE resins.

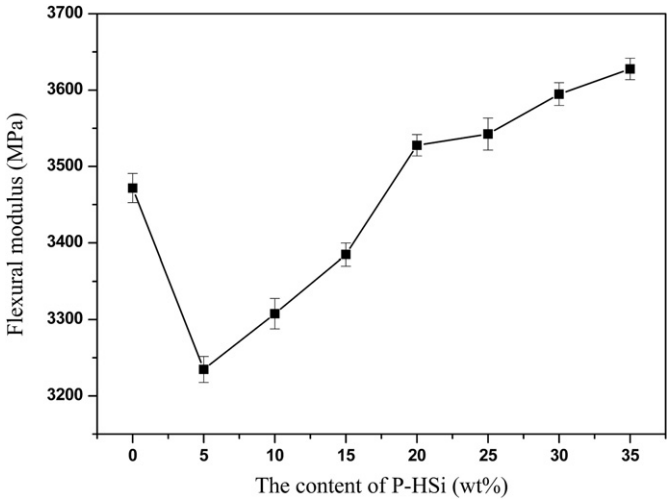

Fig. 14. The flexural moduli of cured CE and P–HSi/CE resins.

The *E'* in glassy state is determined by the secondary valence forces, hence it is dependent on the packing density or concentration of the chain segments in the glassy state [56,57]. Some investigations have proved that the strong π–π electron conjugation interactions will be inevitably occurred for the aromatic rings of heterogenous systems, while the aromatic rings of one system can drive the aromatic rings of another system to move cooperatively, and disrupt the microsegregation of phenyl groups into stacks, as a result, changing the mechanical properties of the system [58,59]. Fig. 15 shows the UV–visible spectra of P–HSi, cured CE and P–HSi15/CE resins. Compared with P–HSi and cured CE resin, P–HSi15/CE resin has higher intensity of the peak assigning to the benzene ring (257 nm), indicating that some cooperative motions occur between benzene rings of both CE and P–HSi resulting from their π–π electron conjugation interactions.

Owing to a large amount of unoccupied structure, a hyperbranched polymer usually has higher average volume of free cavities that play a negative role in decreasing the concentration of the chain segment of modified resins. Meanwhile, in the case of the P–HSi/CE resins, there are strong π–π electron conjugation interactions between P–HSi and CE, which can conspicuously increase the packing density of the polymer. When the content of P–HSi is between 5 and 15 wt%, the negative factor occupies a dominant role. However, when the content of P–HSi is large enough, the improvement in storage and flexural moduli becomes obvious because more π–π electron conjugation interactions occur as the content of P–HSi increases.

3.4.3. Flexural strength

Flexural strength is usually used for evaluating the mechanical properties of a material because the flexural loading is very complicated and may contain multi-type loadings such as tensile, shearing and/or compressing loadings [60]. Therefore, to evaluate the integrated mechanical properties of a material, flexural strength is usually selected as a typical parameter to evaluate the integrated mechanical properties.

The flexural strengths of cured CE and P–HSi/CE resins are shown in Fig. 16. All P–HSi/CE resins have higher flexural strengths than neat CE resin. With increasing the content of P–HSi, the flexural strength of the P–HSi/CE resin initially increases, and then reaches the maximum value (139 MPa) at 15 wt% P–HSi, reflecting a significant improvement in integrated mechanical properties compared with CE resin. Note that the addition of 15 wt% P–HSi will also endow the modified resin with outstanding flame retardancy as discusses later. These interesting results are opposite to those in literature, in detail, a suitable content of phosphorus-containing flame retardant will contribute a satisfactory flame retardancy to a resin, but meanwhile, which usually brings a negative affect on the flexural strength of the resin system [20,61].

Generally, the increased flexural strength of a material primarily arises from the combination of the significant improvement in stiffness and/or toughness, so those factors that are beneficial in improving the stiffness and/or the toughness can improve the flexural strength. A large amount of rigid groups (benzene rings), flexible molecular chains and hydrogen bonds between P═O and –OH of P–HSi are introduced into the CE resin, consequently, the combined role of the three factors leads to the result that P–HSi/CE resins have better flexural strengths than neat CE resin.

3.5. Dielectric property of cured P–HSi/CE resins

The biggest merit of CE resin is its extremely low and stable dielectric loss (0.003–0.006) over a wide range of frequency [62,63], hence it is necessary to investigate the dielectric property of modified CE resin.

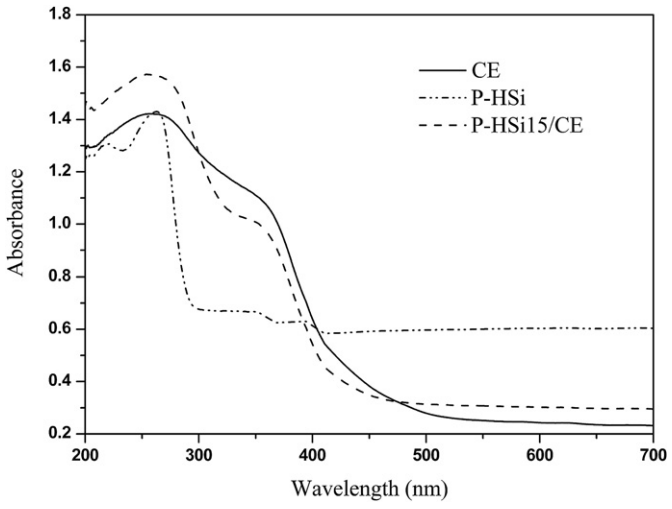

Fig. 15. UV–visible spectra of P–HSi, cured CE and P–HSi15/CE resins.

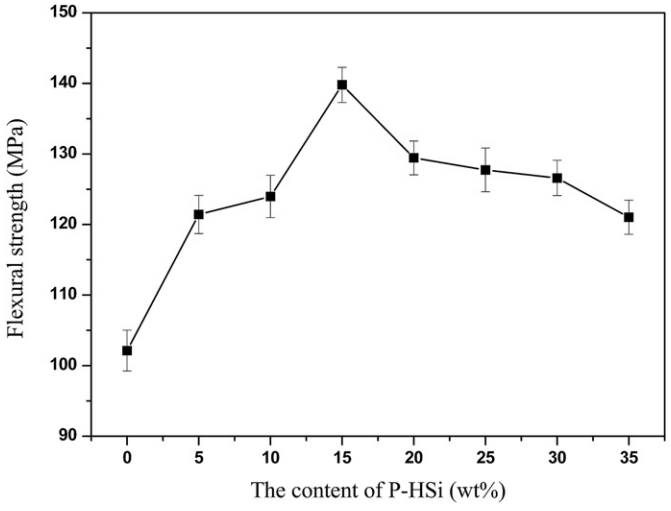

Fig. 16. Flexural strengths of cured CE and P–HSi/CE resins.

Fig. 17 shows dielectric properties of cured CE and P–HSi/CE resins at different frequencies. Compared with CE resin, P–HSi/CE resins have similar dielectric constant as cured CE resin over the whole frequency tested, for example, the dielectric constant at 1 kHz of P–HSi5/CE and P–HSi35/CE resin is 3.17 and 3.28, about 97.2% and 100.6% of that of CE resin, respectively. For the dielectric loss, it can be seen that all P–HSi/CE resins have lower dielectric losses over the whole frequency tested than neat CE resin, for example, the dielectric loss at 1 kHz of P–HSi5/CE resin is 0.0024, about 77% of that of CE resin. The dielectric loss of P–HSi/CE resins enlarges as the content of P–HSi increases, the dielectric loss at 1 kHz of P–HSi35/CE resin is about 96.8% of that of CE resin.

Generally, the dielectric properties of a polymer depend on the orientation and relaxation of dipoles in the applied electric field, the process of dipole polarization accompanies the movement of the polymer chain segments [59], hence the influence of the addition of P–HSi into CE resin on the dielectric properties is dependent on the variety in the chemical structure and crosslinking density. First, DOPO has a bulky pendant moiety and non-coplanar structure, hence the incorporation of DOPO into CE resin will decrease the dielectric constant and loss [64,65], while the chemistry of hyperbranched polysiloxane also tends to reduce the dielectric constant and loss [66], these factors are beneficial to improve the dielectric properties of the modified CE resin. Second, as discussed above, the influence of P–HSi on the crosslinking density of P–HSi/CE resins is closely related to the content of P–HSi, and thus result in the dependence of dielectric properties on the content of P–HSi. Third, the co-polymerization between P–HSi and CE decreases the formation of triazine rings, and brings –OH groups in the network, tending to enlarge the dielectric constant and loss. The resultant role of these factors consequently leads to the data shown in Fig. 17.

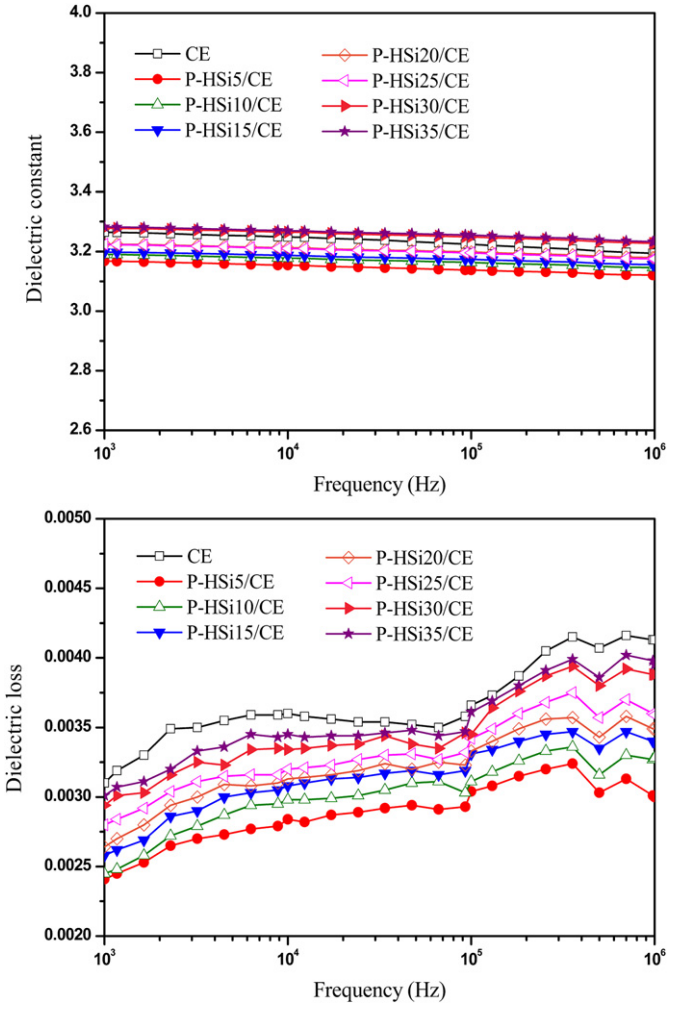

Fig. 17. Dependence of dielectric constant and loss on frequency for cured CE and P–HSi/CE resins.

3.6. Flame retardancy of P–HSi/CE resins

LOI is often used to evaluate the flame retardancy of cured CE and P–HSi/CE resins. As shown in Fig. 18, all modified CE resins have higher LOI values than original resin; moreover, a small addition of P–HSi can effectively improve the flame retardancy of the resin, for example, the LOI value of P–HSi5/CE system is 37%, about 1.3 times of that of CE resin. As the content of P–HSi increases, the LOI value gradually increases and reaches the maximum value (41%, about 1.5 times of the LOI value of the CE resin) at 20 wt% P–HSi, and then almost levels off. This can be attributed to the dependence of the structure of the cured resin on the content of P–HSi as well as the inherent flammability of phosphorus itself [16].

Compared above data with the corresponding values of the resins modified by other hyperbranched polysiloxanes [44,66,67] or the flame retardants containing DOPO and silicon [68] in literature, it is reasonable to state that P–HSi has a super advantage in improving the flame retardancy of a thermosetting resin, reflected by the maximum increasing degree of the flame retardancy, and the increasing degree of the flame retardancy using the same loading of flame retardant. Generally, the maximum increasing degree in flame retardancy of these flame retardants containing DOPO and silicon is1.3 times, which is achieved only when the loading of these flame retardants is as high as 30 wt% [68]; while this degree can be obtained when the content of P–HSi is as low as 5 wt%. On the other hand, the maximum LOI value of a resin modified by a hyperbranched polysiloxane is 1.1–1.3 times of that of the original resin [44,66,67]; while with the addition of 20 wt% P–HSi, the resultant P–HSi/CE resin has the maximum LOI value that is about 1.5 times of that of CE resin.

Fig. 19 shows the SEM micrographs of the surfaces of the residual chars for cured CE and P–HSi15/CE resins after combustion. Different from the residual char of CE resin, that of P–HSi15/CE

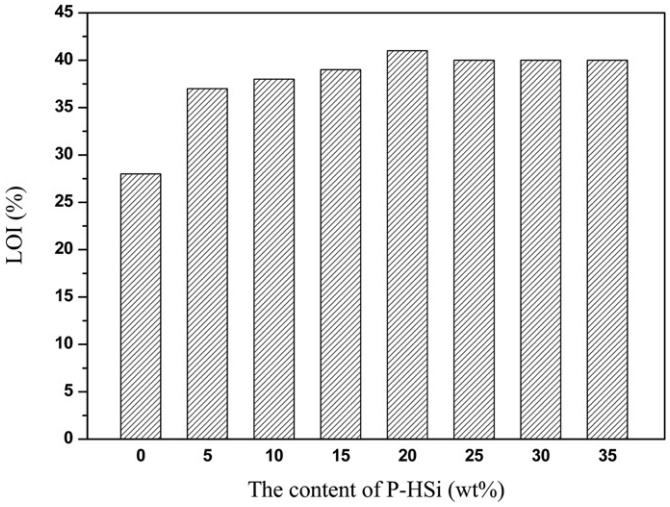

Fig. 18. LOI values of cured CE and P–HSi/CE resins.

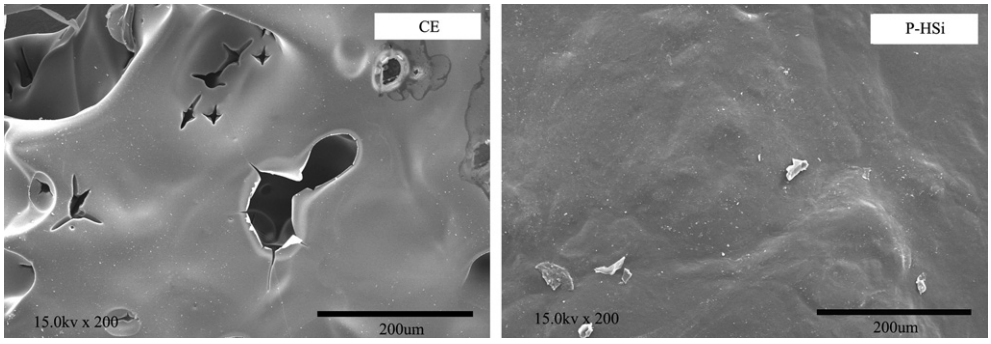

Fig. 19. SEM micrographs of the surfaces of the residual chars for cured CE and P–HSi15/CE resins after combustion.

Table 2
Elemental compositions of the residues for cured CE and P–HSi15/CE resins.

Sample		Elemental composition (wt%)				
		C	N	O	P	Si
Residue of CE	Exterior	89.84	6.49	3.66	0.00	0.00
	Interior	93.08	4.89	2.01	0.00	0.00
Residue of P–HSi15/CE	Exterior	78.81	5.32	8.26	2.13	5.47
	Interior	86.10	6.54	4.26	0.97	2.11

resin is dense, compact and smooth. The corresponding elemental analyses (Table 2) of the residue of P–HSi15/CE resin show that the percents of both P and Si elements in the exterior layer are much larger than those in the interior layer, suggesting that both P and Si elements of P–HSi can migrate toward the surface of the resin, and form a compact layer, which can retard the progress of the flame by not only holding back the flammable gases but also isolating the heat from the unburned resins.

4. Conclusion

A novel phosphorus-containing hyperbranched polysiloxane (P–HSi) with a great amount of DOPO and silanol groups was synthesized. With suitable loadings of P–HSi, the modified CE resins not only have significantly improved flame retardancy, but also much better integrated properties including dielectric properties, thermal stability, toughness, and stiffness. These attractive data suggest that P–HSi completely overcomes the disadvantages of phosphorus-containing flame retardants, and is a multifunctional flame retardant for developing high performance resins.

Acknowledgments

The authors thank Natural Science Foundation of China (21274104, 51173123), the Priority Academic Program Development of Jiangsu Higher Education Institutions (PAPD), the Major Program of Natural Science Fundamental Research Project of Jiangsu Colleges and Universities (11KJA430001), Suzhou Applied Basic Research Program (SYG201141) for financially supporting this project.

References

[1] Laoutid F, Bonnaud L, Alexandre M, Lopez-Cuesta JM, Dubois P. New prospects in flame retardant polymer materials: from fundamentals to nanocomposites. Mater Sci Eng R Rep 2009;63:100–25.
[2] Song P, Zhao L, Cao Z, Fang Z. Polypropylene nanocomposites based on C60-decorated carbon nanotubes: thermal properties, flammability, and mechanical properties. J Mater Chem 2011;21:7782–8.
[3] Ma HY, Tong LF, Xu ZB, Fang ZP. Functionalizing carbon nanotubes by grafting on intumescent flame retardant: nanocomposite synthesis, morphology, rheology, and flammability. Adv Funct Mater 2008;18:414–21.
[4] Yu D, Kleemeier M, Wu GM, Schartel B, Liu WQ, Hartwig A. A low melting organic-inorganic glass and its effect on flame retardancy of clay/epoxy composites. Polymer 2011;52:2120–31.
[5] Yu D, Kleemeier M, Wu GM, Schartel B, Liu WQ, Hartwig A. The absence of size-dependency in flame retarded composites containing low-melting organic-inorganic glass and clay: comparison between micro- and nano-composites. Polym Degrad Stab 2011;96:1616–24.
[6] Nam S, Condon BD, Parikh DV, Zhao Q, Cintrón MS, Madison C. Effect of urea additive on the thermal decomposition of greige cotton nonwoven fabric treated with diammonium phosphate. Polym Degrad Stab 2011;96:2010–8.
[7] Yu D, Kleemeier M, Wu GM, Schartel B, Liu WQ, Hartwig A. Phosphorous and silicon containing low-melting organic-inorganic glasses improve flame retardancy of epoxy/clay composites. Macromol Mater Eng 2011;296:952–64.
[8] Wu GM, Schartel B, Yu D, Kleemeier M, Hartwig A. Synergistic flame retardancy in layered-silicate epoxy nanocomposite combined with low-melting phenysiloxane glass. J Fire Sci 2012;30:69–87.
[9] Pospiech D, Häußler L, Korwitz A, Fischer O, Starke S, Jehnichen D, et al. The miscibility of poly (butylene terephthalate)(PBT) with phosphorus polyester flame retardants. High Perform Polym 2012;24:64–73.
[10] Liao SH, Liu PL, Hsiao MC, Teng CC, Wang CA, Ger MD, et al. One step reduction and functionalization of graphene oxide with phosphorus-based compound to produce flame retardant epoxy nanocomposite. Indus Eng Chem Res 2012; 51(12):4573–81.
[11] Zhong H, Wei P, Jiang P, Wang G. Thermal degradation behaviors and flame retardancy of PC/ABS with novel silicon-containing flame retardant. Fire Mater 2007;31:411–23.
[12] Schartel B, Braun U, Balabanovich A, Artner J, Ciesielski M, Döring M, et al. Pyrolysis and fire behaviour of epoxy systems containing a novel 9, 10-dihydro-9-oxa-10-phosphaphenanthrene -10-oxide-(DOPO)-based diamino hardener. Eur Polym J 2008;44:704–15.
[13] Qian LJ, Ye LJ, Xu GZ, Liu J, Guo JQ. The non-halogen flame retardant epoxy resin based on a novel compound with phosphaphenanthrene and cyclotriphosphazene double functional groups. Polym Degrad Stab 2011;96:1118–24.
[14] Chen X, Gu A, Liang G, Yuan L, Zhuo D, Hu J. Novel low phosphorus-content bismaleimide resin system with outstanding flame retardancy and low dielectric loss. Polym Degrad Stab 2012;97:698–706.
[15] Schartel B, Balabanovich AI, Braun U, Knoll U, Artner J, Ciesielski M, et al. Pyrolysis of epoxy resins and fire behaviour of epoxy resin composites flame-retarded with 9,10-dihydro-9-oxa-10-phosphaphenanthrene-10 -oxide additives. J Appl Polym Sci 2007;104:2260–9.
[16] Brehme S, Schartel B, Goebbels J, Fischer O, Pospiech D, Bykov Y, et al. Phosphorus polyester versus aluminium phosphinate in poly(butylene terephthalate) (PBT): flame retardancy performance and mechanisms. Polym Degrad Stab 2011;96:875–84.
[17] Perret B, Schartel B, Stöß K, Ciesielski M, Diederichs J, Döring M, et al. A new halogen-free flame retardant based on 9,10-dihydro-9-oxa-10-phosphaphenanthrene-10-oxide for epoxy resins and their carbon fiber composites for the automotive and aviation industries. Macromol Mater Eng 2011;296:14–30.
[18] Perret B, Schartel B, Stöß K, Ciesielski M, Diederichs J, Döring M, et al. Novel DOPO-based flame retardants in high-performance carbon fibre epoxy composites for aviation. Eur Polym J 2011;47:1081–9.
[19] Wang X, Hu Y, Song L, Yang H, Xing W, Lu H. Synthesis and characterization of a DOPO-substitued organophosphorus oligomer and its application in flame retardant epoxy resins. Prog Organ Coat 2011;71:72–82.
[20] Chen ZK, Yang G, Yang JP, Fu SY, Ye L, Huang YG. Simultaneously increasing cryogenic strength, ductility and impact resistance of epoxy resins modified by n-butyl glycidyl ether. Polymer 2009;50:1316–23.
[21] Zhang S, Li B, Lin M, Li Q, Gao S, Yi W. Effect of a novel phosphorus-containing compound on the flame retardancy and thermal degradation of intumescent flame retardant polypropylene. J Appl Polym Sci 2011;122:3430–9.

[22] Lin JS, Liu Y, Wang DY, Qing Q, Wang YZ. Poly (vinyl alcohol)/ammonium polyphosphate systems improved simultaneously both fire retardancy and mechanical properties by montmorillonite. Indus Eng Chem Res 2011;50: 9998–10005.
[23] Yan L, Zheng Y, Liu J, Shang H. Synthesis of polymeric flame retardants containing phosphorus-nitrogen-bromide and their application in acrylonitrile-butadiene-styrene. J Appl Polym Sci 2010;115:957–62.
[24] Zhuo D, Gu A, Liang G, Hu J, Yuan L, Chen X. Flame retardancy materials based on a novel fully end-capped hyperbranched polysiloxane and bismaleimide/diallylbisphenol A resin with simultaneously improved integrated performance. J Mater Chem 2011;21:6584–94.
[25] Anuradha G, Sarojadevi M. Synthesis and characterization of poly (arylene ether) containing cyanate ester networks. J Polym Res 2008;15:507–14.
[26] Guan Q, Gu A, Liang G, Zhou C, Yuan L. Preparation and properties of new high performance maleimide-triazine resins for resin transfer molding. Polym Adv Techno 2011;22:1572–80.
[27] Zhang X, Gu A, Liang G, Zhuo D, Yuan L. Liquid crystalline epoxy resin modified cyanate ester for high performance electronic packaging. J Polym Res 2011;18:1441–50.
[28] Wang CS, Shieh JY, Sun YM. Synthesis and properties of phosphorus containing PET and PEN (I). J Appl Polym Sci 1998;70:1959–64.
[29] Qian LJ, Ye LJ, Qiu Y, Qu S. Thermal degradation behavior of the compound containing phosphaphenanthrene and phosphazene groups and its flame retardant mechanism on epoxy resin. Polymer 2011;52:5486–93.
[30] Kariuki BM, Harris KDM, Philp D, Robinson JMA. A triphenylphoshine oxide-water aggregate facilitates an exceptionally short CH. O hydrogen bond. J Am Chem Soc 1997;119:12679–80.
[31] Steiner T. The hydrogen bond in the solid state. Angew Chem Intern Edit 2002;41:48–76.
[32] Sung CSP, Schneider NS. Temperature dependence of hydrogen bonding in toluene diisocyanate based polyurethanes. Macromolecules 1977;10:452–8.
[33] Teo LS, Chen CY, Kuo JF. Fourier transform infrared spectroscopy study on effects of temperature on hydrogen bonding in amine-containing polyurethanes and poly(urethne-urea)s. Macromolecules 1997;30:1793–9.
[34] Potrzebowski MJ, Kazmierski S, Kassassir H, Miksa B. Phosphorus-31 NMR spectroscopy of condensed matter. Ann Rep NMR Spectrosc 2010;70:35–114.
[35] Hölter D, Burgath A, Frey H. Degree of branching in hyperbranched polymers. Acta Polym 1997;48:30–5.
[36] Osei-Owusu A, Martin G, Gotro J. Analysis of the curing behavior of cyanate ester resin systems. Polym Eng Sci 1991;31:1604–9.
[37] Santhosh Kumar K, Reghunadhan Nair C, Ninan K. Investigations on the cure chemistry and polymer properties of benzoxazine-cyanate ester blends. Eur Polym J 2009;45:494–502.
[38] Kaynak C, Celikbilek C, Akovali G. Use of silane coupling agents to improve epoxy–rubber interface. Eur Polym J 2003;39:1125–32.
[39] Ardhyananta H, Wahid MH, Sasaki M, Agag T, Kawauchi T, Ismail H, et al. Performance enhancement of polybenzoxazine by hybridization with polysiloxane. Polymer 2008;49:4585–91.
[40] Schütz MR, Sattler K, Deeken S, Klein O, Adasch V, Liebscher CH, et al. Improvement of thermal and mechanical properties of a phenolic resin nanocomposite by in situ formation of silsesquioxanes from a molecular precursor. J Appl Polym Sci 2010;117:2272–7.
[41] Ward IM, Sweeney J. An introduction to the mechanical properties of solid polymers. New York: Wiley & Sons Inc; 1993.
[42] Juang TY, Liu JK, Chang CC, Shau SM, Tsai MH, Dai SA, et al. A reactive modifier that enhances the thermal mechanical properties of epoxy resin through the formation of multiple hydrogen-bonded network. J Polym Res 2011;18:1169–76.
[43] Wang X, Hu Y, Song L, Xing W, Lu H. Preparation, mechanical properties, and thermal degradation of flame retarded epoxy resins with an organophosphorus oligomer. Polym Bull 2011;67:859–73.
[44] Zhou C, Gu A, Liang G, Yuan L. Novel toughened cyanate ester resin with good dielectric properties and thermal stability by copolymerizing with hyperbranched polysiloxane and epoxy resin. Polym Adv Tech 2011;22:710–7.
[45] Bussu G, Lazzeri A. On the use of dynamic mechanical thermal analysis (DMTA) for measuring glass transition temperature of polymer matrix fibre reinforced composites. J Mater Sci 2006;41:6072–6.
[46] Ji L, Gu A, Liang G, Yuan L. Novel modification of bismaleimide–triazine resin by reactive hyperbranched polysiloxane. J Mater Sci 2010;45:1859–65.
[47] Perez R, Sandler J, Altstädt V, Hoffmann T, Pospiech D, Artner J, et al. Novel phosphorus-containing hardeners with tailored chemical structures for epoxy resins: synthesis and cured resin properties. J Appl Polym Sci 2007;105: 2744–59.
[48] Hawker CJ, Chu F. Hyperbranched poly (ether ketones): manipulation of structure and physical properties. Macromolecules 1996;29:4370–80.
[49] Ward IM, Ward I. Mechanical properties of solid polymers. New York: Wiley; 1983.
[50] Yang JP, Chen ZK, Yang G, Fu SY, Ye L. Simultaneous improvements in the cryogenic tensile strength, ductility and impact strength of epoxy resins by a hyperbranched polymer. Polymer 2008;49:3168–75.
[51] Lv S, Yuan Y, Shi W. Strengthening and toughening effects of layered double hydroxide and hyperbranched polymer on epoxy resin. Prog Organ Coat 2009;65:425–30.
[52] Foix D, Serra A, Amparore L, Sangermano M. Impact resistance enhancement by adding epoxy ended hyperbranched polyester to *DGEBA* photocured thermosets. Polymer 2012;53:3084–8.
[53] Lee-Sullivan P, Dykeman D. Guidelines for performing storage modulus measurements using the TA Instruments DMA 2980 three-point bend mode: I. Amplitude effects. Polym Test 2000;19:155–64.
[54] Karthikeyan C, Sankaran S. Investigation of bending modulus of fiber-reinforced syntactic foams for sandwich and structural applications. Polym Adv Tech 2007;18:254–6.
[55] Shao Q, Lee-Sullivan P. Guidelines for performing storage modulus measurements using the TA Instruments DMA 2980 three-point bend mode II. Contact stresses and machine compliance. Polym Test 2000;19:239–50.
[56] Meares P. Polymers: structure and bulk properties. London and New York: Van Nostrand; 1965.
[57] Meijer HEH, Govaert LE. Mechanical performance of polymer systems: the relation between structure and properties. Prog Polym Sci 2005;30: 915–38.
[58] Feng H, Feng Z, Ruan H, Shen L. A high-resolution solid-state NMR study of the miscibility, morphology, and toughening mechanism of polystyrene with poly (2, 6-dimethyl-1, 4-phenylene oxide) blends. Macromolecules 1992;25: 5981–5.
[59] Kambour R, Gundlach P, Wang ICW, White D, Yeager G. Miscibility of poly (2, 6-dimethyl-1, 4-phenylene oxide) with several styrenic homopolymers: dependence of interaction parameters from critical molecular weights on cohesive energy densities. Polym Commun 1988;29:170–2.
[60] Xavier S, Misra A. Influence of glass fiber content on the morphology and mechanical properties in injection molded polypropylene composites. Polym Compos 1985;6:93–9.
[61] Li B, He J. Investigation of mechanical property, flame retardancy and thermal degradation of LLDPE–wood-fibre composites. Polym Degrad Stab 2004;83: 241–6.
[62] Liang K, Toghiani H, Li G, Pittman Jr CU. Synthesis, morphology, and viscoelastic properties of cyanate ester/polyhedral oligomeric silsesquioxane nanocomposites. J Polym Sci Polym Chem 2005;43:3887–98.
[63] Wooster TJ, Abrol S, Hey JM, MacFarlane DR. Thermal, mechanical, and conductivity properties of cyanate ester composites. Compos Pt A Appl S 2004;35:75–82.
[64] Spontón M, Lligadas G, Ronda J, Galià M, Cádiz V. Development of a DOPO-containing benzoxazine and its high-performance flame retardant copolybenzoxazines. Polym Degrad Stab 2009;94:1693–9.
[65] Lin CH, Cai SX. Flame-retardant epoxy resins with high glass-transition temperatures. II. Using a novel hexafunctional curing agent: 9, 10-dihydro-9-oxa-10-phosphaphenanthrene 10-yl-tris (4-aminophenyl) methane. J Polym Sci Polym Chem 2005;43:5971–86.
[66] Zhuo D, Gu A, Liang G, Hu J, Cao L, Yuan L. Flame retardancy and flame retarding mechanism of high performance hyperbranched polysiloxane modified bismaleimide/cyanate ester resin. Polym Degrad Stab 2011;96: 505–14.
[67] Zhuo D, Gu A, Liang G, Hu J, Zhou C, Yuan L. Modified cyanate ester resins with lower dielectric loss, improved thermal stability, and flame retardancy. Polym Adv Technol 2011;22:2617–25.
[68] Zhong H, Wu D, Wei P, Jiang P, Li Q, Hao J. Synthesis, characteristic of a novel additive-type flame retardant containing silicon and its application in PC/ABS alloy. J Mater Sci 2007;42:10106–12.